Relaxation and Contrast Mechanisms in Living Tissue

Greg J Stanisz
Imaging Research Sunnybrook & Women's College Health Sciences Centre
Department of Medical Biophysics, University of Toronto
stanisz@sw.ca

Introduction

MR images provide unique visual distinction between different types of tissue and tissue pathology, allowing for spectacular visualization of human anatomy *in vivo*. Moreover, due to the unique nature of the MRI signal, it is possible to alter the image contrast in order to maximize the visual information in different regions of human body. Most tissues consist of 75±15% water and because there are two hydrogen nuclei per water molecule, the proton MR signal from tissues is primarily due to protons located in water molecules. In principle, the MR signal from many other macromolecules (lipids and proteins, fat) should also be readily observable since they have approximately the same proton content. Unfortunately, protons associated with these molecules exhibit very short T2 relaxation times and therefore they are MRI "invisible". However, the presence of large macromolecules and cell membranes significantly influences water protons macromolecular dynamics resulting in distinct MR characteristics of water in tissue.

The MR signal is dependent on the physical and chemical processes experienced by protons associated with water molecules in tissue. In general, the MRI signal is a measure of total magnetization, M, which is a vector sum of the individual spins and in consequence depends on the interactions between water protons, external magnetic field, B_0 and tissue microenvironment. In particular, MRI magnetization depends on:

$$M = M(\rho, T_1, T_2, B_{EFF}, T, geometry, environment....) \qquad [1]$$

where: ρ denotes water protons spin density (proportional to the number of spins), $T_{1,2}$ are the longitudinal and transverse relaxation time constants. B_{EFF} denotes effective magnetic field experienced by the individual spins and depends on spatial and temporal magnetic field fluctuations in the tissue. Tissue heterogeneity and the presence of macromolecules significantly affects MR signal. Equation 1 demonstrates complexity of the MR contrast mechanisms in tissues and also shows MR sensitivity to tissue microstructure and composition. It is precisely this complexity and sensititivity that makes MRI such a successful imaging modality. In this lecture, the different contrast mechanisms in tissues will be discussed in some detail.

T_1 and T_2 relaxation

The investigation of the relaxation processes of water in tissues has a rich history and spans several decades (prior to MRI). In the 1950's Shaw [1] and Odeblad [2] used proton NMR measurements to determine water content and other simple biophysical parameters. The relationship of molecular motions to relaxation characteristics is based on the theory of Bloembergen, Purcell and Pound (BPP) published in 1948 [3] which forms the foundation for the understanding of relaxation mechanisms. However, BPP theory alone offers only a qualitative description of water molecular dynamics in tissues (Fig.1). This is because of the presence of many types of macromolecules and cell membranes that result in continuum spectrum of correlation times. According to BPP, T1 relaxation time strongly increases with the magnetic field whereas T2 should remain relatively constant. This field dependence is presented for variety of tissues in Table 1.

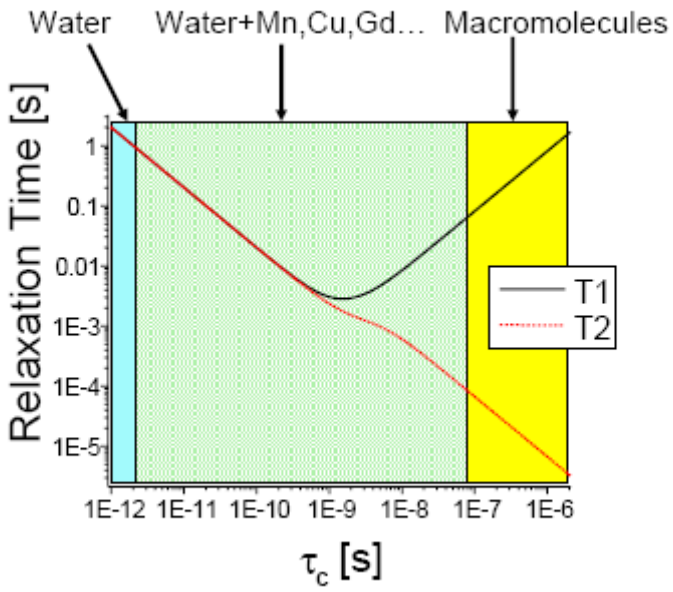

Figure 1. T1 and T2 relaxation as a function of molecular motion (correlation time) according to BPP theory.

Table 1. T_2 and T_1 relaxation times at 3T and 1.5T measured at 37°C. Literature data is also shown.

Tissue	T_2 - 3 T [ms]		T_1 – 3 T [ms]		T_2 – 1.5 T [ms]		T_1 – 1.5 T [ms]	
	This study	literature	This study	literature	This study	literature	This study	literature
Liver	42 ± 3		812 ± 64		46 ± 6	54 ± 8[4]	576± 30	~600[5]
Skeletal Muscle	50 ± 4	32 ± 2[6]	1412 ± 13	1420 ±38[6]	44 ± 6	35±4[6]	1008 ± 20	1060 ± 155[6]
Heart	47 ±11		1471 ± 31		40 ± 6	44±6[7]	1030±34	
Kidney	56 ± 4		1194 ± 27		55 ± 3	61±11[8]	690 ±30	709±60[8]
Cartilage 0°	27 ± 3	37 ± 4[6] 45 - 67[9]	1168 ± 18	~1240[6]	30 ± 4	42 ± 7[6]	1024 ± 70	~1060[6]
Cartilage 55°	43 ± 2		1156 ± 10		44 ± 5		1038 ± 67	
White matter	69 ± 3		1084 + 45	1110 ±45[10]	72 ± 4	79 ± 8[11]	884 ± 50	778 ± 84[11]
Grey matter	99 ± 7		1820 ± 114	1470± 50[10]	95 ± 8	~95[12]	1124 ± 50	1086 ± 228[11]
Optic Nerve	78 ± 5		1083 ± 39		77 ± 9		815 ± 30	
Spinal Cord	78 ± 2		993 ± 47		74 ± 6		745 ± 37	
Blood	275 ± 50		1932 ± 85	~1550[13]	290 ± 30	327± 40[14]	1441 ± 120	~1200[13]

There is a substantial discrepancy in literature concerning T_2 relaxation time and its "apparent" decrease with magnetic field. By definition, the transverse relaxation time, T_2 results from time-dependent variations of the effective magnetic field "seen" by an average proton in the measured system. This classical T_2 characteristic (intrinsic T_2 relaxation time) takes into account rotational and diffusional motion of protons in

tissue. It does not, however, include spatially varying magnetic fields. In particular, the presence of paramagnetic or supermagnetic (iron) particles or altered tissue susceptibility result in microscopic field variations that may not be easily compensated by spin echo (or CPMG) sequence. Therefore, measured T_2 relaxation time may depend on the external magnetic field and more importantly on the echo time, TE. It is not surprising therefore, to observe some decrease in measured literature T_2 values at sufficiently long echo times. In the case of tissue devoid of paramagnetic impurities, measured T_2 represents an intrinsic T_2 value. For example, in the case of white matter, the T_2 relaxation spectra do not depend on TE or field strength (data not shown). Moreover, accurate T_2 relaxation time estimation relies on the accuracy of 180^0 pulses, which are not perfect in typical MR imaging. Finally, the T_2 relaxation in tissues is typically not mono-exponential. Therefore, the evaluated, apparent T_2 relaxation time (typically based on two TE values) depends on the TE chosen for final analysis (Dr Alex MacKay – private communication). In summary, the quantitative assessment of the T_2 relaxation time should be considered with caution.

Tissue Compartments and Exchange

Due to structural heterogeneity contrast mechanisms in tissue are often complex. It is common to approximate tissue microstructure using multi-compartmental tissue models (Fig.2).

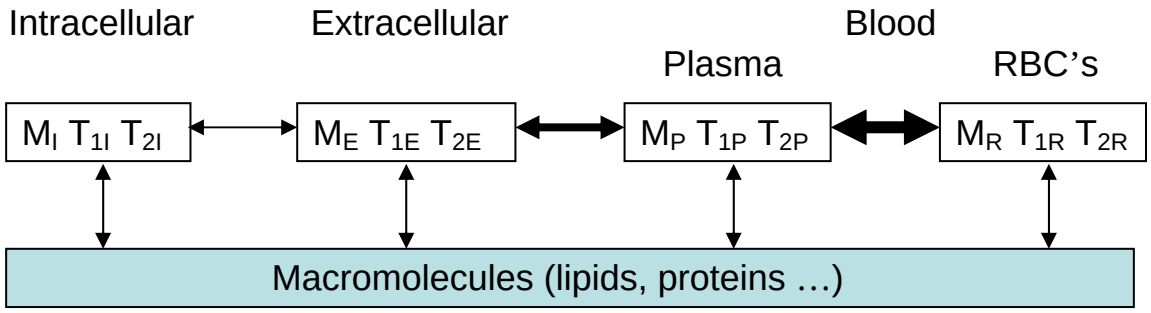

Figure 2. Compartmental model of tissue. Each compartment has its own magnetization, M and intrinsic longitudinal, T_1 and transverse, T_2 relaxation times. The spins are allowed to exchange (arrows) between tissue compartments. The macromolecular pool is not "visible" in a standard MRI experiment , due to its extremely short T_2 relaxation (in order of μs [15]). However, it may significantly influence MR parameters of "visible" liquid protons in intra, extra and blood compartments

Since the physical environment of water in different tissue compartments is vastly different, there is no reason to believe that the intrinsic relaxation times in tissue compartments are similar. For example T_2 relaxation of red blood cell (RBC) is in order of 130 ms [14], whereas T_2 of plasma is inapproximately 700 ms. Therefore, one may expect multi-exponential behavior of T_2 or T_1 relaxation tissue. In particular, T_2 relaxation could be expressed as:

$$M(t) = \sum_k M_k \exp(-t / T_{2k}) \quad [2]$$

where k denotes various tissue compartments. Figure 3 shows typical, non-monoexponential T_2 data showing the complexity of T_2 relaxation decay.

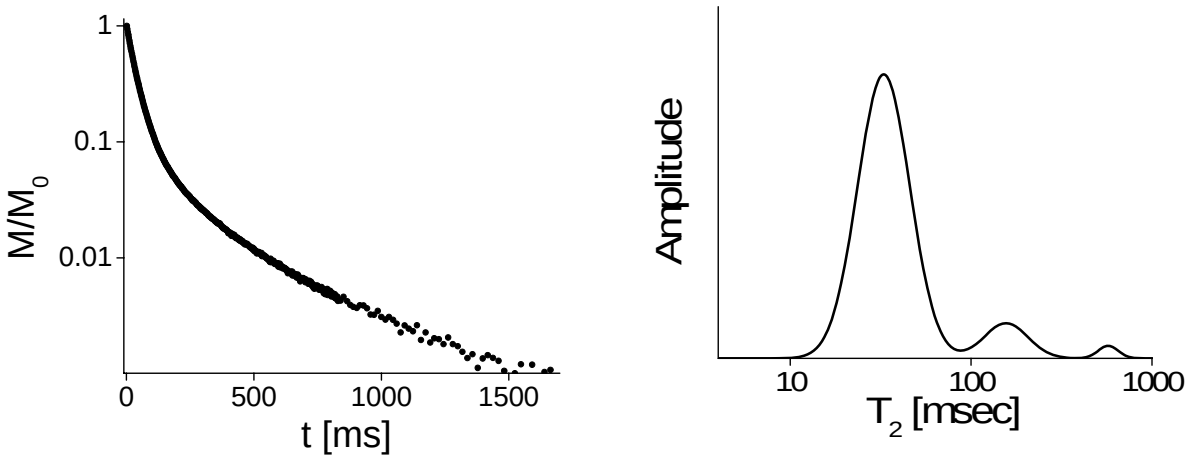

Figure 3. T_2 decay data for muscle tissue (left) is multicomponent and thus appears upwardly curving on a logarithmic plot. T_2 decay data is analyzed using a non-negative-least squares (NNLS) algorithm [16]resulting in a fitted T_2 spectrum (right) which shows, as a function of T_2 relaxation, the relative signal amplitude.

The physical interpretation of the relaxation decay is however, much more complex than eq. [2] would indicate. This is because of the exchange of protons between various tissue compartments. On the typical scale of the MR experiment (~hundreds of ms) the water proton can migrate from one tissue compartment to the other or exchange its spins with immobile protons associated with macromolecules.
The processes of inter-compartmental exchange have been shown to have a profound effect on MR measures of tissue such as T_1 and T_2 and diffusion. The exchange process can be easily incorporated into the standard Bloch equations describing the magnetization behavior. For example for the simplest case of the two-compartmental system consisting of intra and extracellular water the magnetization of each of the pools can be described as:

$$\frac{dM_I}{dt} = -R_I M_I - k_{IE} M_I + k_{EI} M_E \qquad [3]$$
$$\frac{dM_E}{dt} = -R_E M_E + k_{IE} M_I - k_{EI} M_E$$

where $M_{I,E}$ denote the magnetization in intra (I) and extracellular (E) space, $R_{I,E}$ the rates of decay (1/T2) and k_{EI} exchange ratio from extracellular to intracellular space, which has to satisfy the boundary condition, in order to preserve the spin densities in intra- and extracellular space:

$$M_I(0)k_{IE} = M_E(0)k_{EI} \qquad [4]$$

$M_{I,E}(0)$ denote equilibrium magnetization in each of the pools. Eqs. 3-4 can be readily solved, showing that the total magnetization of two-compartmental system (M_I+M_E) decays bi-exponentially with two well distinguished rates that are illustrated in Fig.4. In the absence of exchange ($k_{IE}=0$) the total magnetization is characterized by two relaxation rates that are equal to the intrinsic decay rates $R_{I,E}$ of intra and extracellular pools. The relative amplitudes of those decay rates are also equal to the populations of the intra and extracellular compartments (Fig.4a). However, when the exchange is present both the decay rates and their relative amplitudes are <u>not</u> equal to the intrinsic ones as shown in Fig.4b. Finally, when the exchange rate is very fast the system decays mono-

exponentially with the rate that is equal to the weighted average of intrinsic rates $R=(M_I*R_I+ME*R_e)/(M_I+M_E)$. This scenario is often described in terms of three exchange regimes [17, 18]:

a) Slow ($R_{I,E}>>k_{IE}$)
b) Intermediate ($R_{I,E}\sim k_{IE}$)
c) Fast ($R_{I,E}<<k_{IE}$)

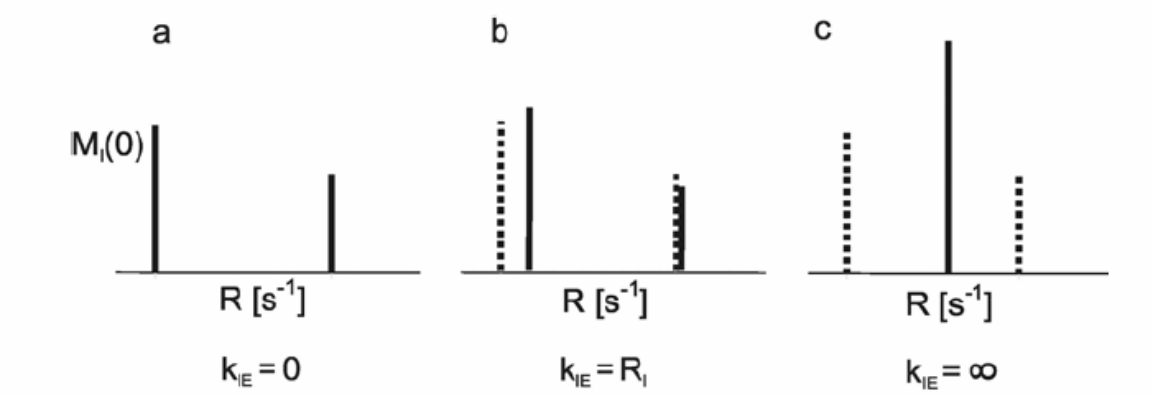

Figure 4. The relaxation components of two-pool model system in the case of negligible (a), intermediate (b) and fast exchange (c). The dotted lines represent intrinsic relaxation rates of two pools. Note that both the amplitudes and positions of relaxation rates, in the presence of exchange do not correspond to the intrinsic ones. In the case of the fast exchange regime the system decays with single relaxation rate constant that is weighted average of

The exchange process between liquid tissue compartments (intra-, extracellular, plasma and blood) is thought to be mediated by the process of water molecule diffusion through the semi-permeable membranes [19]. It is common to express cell membrane permeability, P, in the terms of the pseudo-first order exchange rate k_{IE}:

$$k_{IE} = P\frac{S}{V} \qquad [4]$$

where S/V is a surface-to-volume ratio of the cell. The cell membrane permeability, P, depends on the type of cell membrane and the mobility of water inside the cell. The literature data concerning cell membrane permeability for water are very limited and P is only accurately known for RBC (2.5–3.0) x 10^{-3} cm s^{-1} [19] . For other types of cells, P is estimated to be lower than that of RBC, but in most cases larger than 0.5 x10^{-3} cm s^{-1}. *In vitro* MRI experiments in bovine optic nerve estimated axonal and glial permeability at (0.9 ± 0.2) and (1.7 ± 0.3) x10^{-3} cm s^{-1}, respectively [20].

The inverse of k_{IE} defines the average residence time, τ, of the water molecule inside the cell. It is therefore evident that the exchange rate constant (thus τ) depends not only on P, but also on cellular size and cell shape. It is apparent that water inside cells with small diameter has a relatively short τ . In contrast, τ is large for large cells. It is to be expected, since for the larger cellular size, it would take longer for an average water molecule to reach the cell membrane and eventually cross it. τ has been estimated previously to range from approximately 12 ms for RBC [21], to 600 ms for neuronal cells [22].

Magnetization Transfer

Water spins also interact with protons associated with macromolecules in tissues. This interaction is also often expressed in terms of magnetization transfer (MT) [23] also known as the Nuclear Overhauser Effect (NOE). In this case however, the spin interactions are mediated by chemical (exchange of protons between water and

macromolecule) or physical (dipolar spin) exchange. The mathematical formalism, however is very similar to that for inter-compartmental diffusion exchange [24]. Figure 5 shows a two-pool model that is simple yet sufficient for quantitative interpretation of MT.

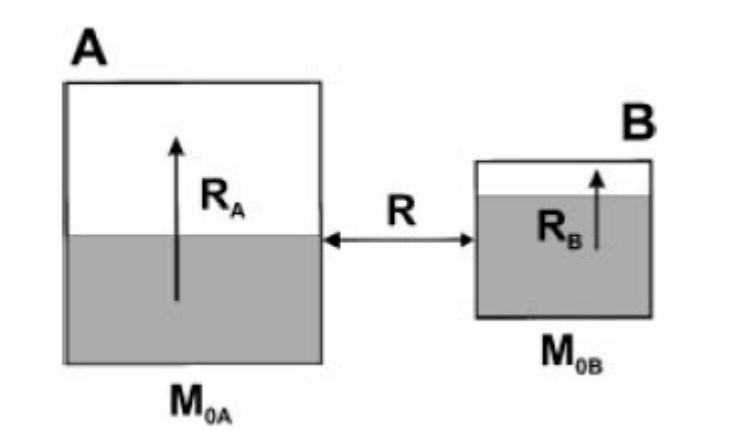

Figure 5. A two-pool model of magnetization transfer exchange. The shaded region in each pool represents saturated spins. R_A and R_B represent longitudinal relaxation rates ($1/T_1$) in liquid in macromolecular pool. R denotes magnetization transfer exchange.

Pool A represents the liquid spins. The number of spins in this compartment is by convention normalized to unity ($M_{0A} = 1$). Pool B represents the macromolecular spins. In tissues, the number of macromolecular spins is much less than the liquid spins and the relative fraction is given by M_{0B} and is typically on the order of a few percent. In each pool, and at any instant in time, some of the spins are in the longitudinal orientation represented by the upper un-shaded portion of the compartment and some spins are saturated, represented by the lower shaded portion. The partition into longitudinal spins and saturated spins depends on the prior irradiation history. In the typical MT experiment the off-resonance saturation pulse is applied. The effect of off-resonance irradiation on this system is different for the two pools. For pool B, the protons in the macromolecules are strongly coupled to each other resulting in a homogeneously broadened absorption lineshape. Thus, off-resonance irradiation results in progressive saturation of the ensemble of spins, with the effective saturation rate being given by the probability of absorption at the corresponding offset frequency times the average radio frequency (RF) power at the offset frequency. In MT experiments, the intent is to manipulate the liquid pool indirectly by saturating the macromolecular pool. However, some direct saturation of the liquid pool is inevitable in this process and must be included in any quantitative analysis of MT effects. The MT data is often presented as a Z-spectrum [25] shown in Fig.6.

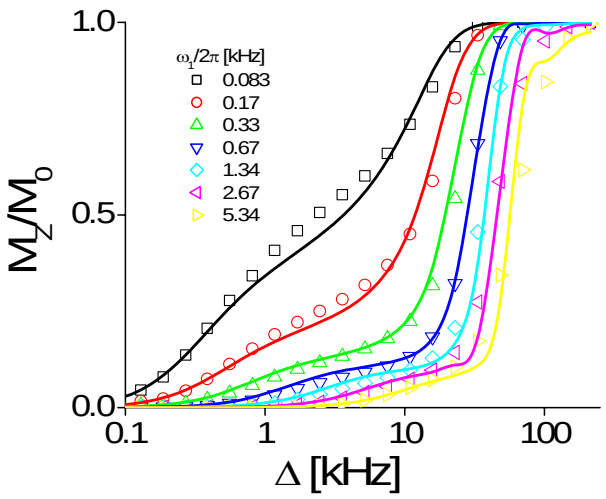

Figure 6. MT experiment for white matter. Normalized residual longitudinal magnetization is plotted versus the frequency offset of the RF saturation pulse. Data for seven different rf amplitudes is shown. The solid lines are the fit of two-pool MT model to the experimental data.

Conclusion

Contrast mechanisms in tissues are quite complex due to high degree of heterogeneity. Quantitative MRI experiments are capable of revealing information about the intrinsic characteristics of protons in different tissue compartments and inter-compartmental exchange.

References

1. Shaw TM, E. RH, and K. CH, *Proton magnetic resonance absorption and water content of biological materials.* Physiol Rev, 1953. 85: p. 708.
2. Odeblad E and L. G, *Some preliminary observation on PMR in biological samples.* Acta Radiol, 1955. 43: p. 469.
3. Bloembergen, N., E. Purcell, and R. Pound, *Relaxation effects in Nuclear Magnetic Resonance Absorption.* Phys Rev, 1948. 73: p. 679-712.
4. Cieszanowski A, et al., *Discrimination of benign from malignant hepatic lesions based on their T2-relaxation times calculated from moderately T2-weighted turbo SE sequence.* Eur Radiol, 2002. 12(9): p. 2273-2279.
5. Graham, S.J., et al., *Analysis of changes in MR properties of tissues after heat treatment.* Magn.reson.Med., 1999. 42: p. 1061-1071.
6. Gold, G., et al., *Musculoskeletal MRI at 3.0T: Relaxation Times and Image Contrast.* Am J Neuroradiol, 2004. 183: p. 343-350.
7. Allmann KH, et al., *MR imaging of the carpal tunnel.* Eur.J.Radiol. 25: p. 141-145.
8. Aherne, T., et al., *Magnetic resonance imaging of cardiac transplants: the evaluation of rejection of cardiac allografts with and without immunosuppression.* Circulation, 1986. 74: p. 145-156.
9. Smith, H., et al., *Spatial Variation in Cartilage T2 of the Knee.* J Magn Reson Imag, 2001. 14(1): p. 50-55.

10. Ethofer, T., et al., *Comparison of Longitudinal Metabolite Relaxation Times in Different Regions of the Human Brain at 1.5 and 3 Tesla.* Magn Res Med, 2003. 50: p. 1296-1301.
11. Sled JG and Pike GB, *Quantitative imaging of magnetization transfer exchange and relaxation properties in vivo using MRI.* Magn Reson Med, 2001. 46: p. 923-932.
12. Pell, G., et al., *Voxel-based relaxometry: a new approach for analysis of T2 relaxometry changes in epilepsy.* Neuroimage, 2004. 21(2): p. 707-713.
13. Greenman, R., et al., *Double inversion black-blood fast spin-echo imaging of the human heart: A comparison between 1.5T and 3.0T.* J Magn Reson Imag, 2003. 17: p. 648-655.
14. Stanisz, G.J., et al., *Water dynamics in human blood via combined measurements of T2 relaxation and diffusion in the presence of gadolinium.* Magn. Reson.Med., 1998. 39: p. 223-233.
15. Henkelman RM, Stanisz GJ, and Graham JS, *Magnetization transfer in MRI: a review.* NMR in Biomed, 2001. 14: p. 57-64.
16. Whittall KP and MacKay AL, *Quantitative interpretation of NMR relaxation data.* J Magn Reson, 1989. 95: p. 134.
17. Dailey AT, et al., *Magnetic resonance neurography of peripheral nerve degeneration and regeneration.* Lancet, 1997. 350: p. 1221-1222.
18. Donahue, K., R. Weisskoff , and D. Burstein, *Water diffusion and exchange as they influence contrast enhancement.* J Magn Reson Imag, 1997. 7: p. 102-110.
19. Andrasko, J., *Water diffusion permeability of human erythrocytes studied by a pulsed gradient NMR technique.* Biochim Biophys Acta, 1976. 428: p. 304-311.
20. Stanisz, G., *Diffusion MR in Biological Systems: Tissue Compartments and Exchange.* Israel J Chem, 2003. 43: p. 33-44.
21. Li, J.G., G.J. Stanisz, and R.M. Henkelman, *Integrated analysis of diffusion and relaxation of water in blood.* Magn Res Med, 1998. 40: p. 79-88.
22. Landis, C., et al., *Determination of the MRI Contrast Agent Concentration Time Course In Vivo Following Bolus Injection: Efffect of Equilibrium Transcytolemmal Water Exchange.* Magn Reson Med, 2000. 44: p. 563-574.
23. Wolff, S. and R. Balaban, *Magnetization Transfer Contrast (MTC) and Tissue Water Proton Relaxation In Vivo.* Magn Reson Imag, 1989. 10: p. 135-144.
24. Henkelman, R.M., et al., *Quantitative interpretation of magnetization transfer.* Magn Reson Med, 1993. 29: p. 759-766.
25. Grad, J. and R. Bryant, *Nuclear magnetic cross-relaxation spectroscopy.* J Magn Reson, 1990. 90: p. 1-8.